Journal of The Electrochemical Society, **157** (4) D187-D192 (2010)
0013-4651/2010/157(4)/D187/6/$28.00 © The Electrochemical Society

A Study on Seed Damage in Plating Electrolyte and Its Repairing in Cu Damascene Metallization

Sung Ki Cho,[a,*] Taeho Lim,[a,] Hong-Kee Lee,[b] and Jae Jeong Kim[a,*,z]**

[a]*Research Center for Energy Conversion and Storage, School of Chemical and Biological Engineering, Seoul National University, Seoul 151-744, Korea*
[b]*Incheon Technology Service Division, Korea Institute of Industrial Technology, Incheon 406-840, Korea*

In this study, we observed the changes in the film properties of a Cu seed layer with its damage and repair. The immersion of the Cu seed layer in a sulfuric-acid-based plating electrolyte can result in damage to the Cu seed layer by the dissolution of the native Cu oxide and corrosion of Cu, leading to defects in the subsequent electrodeposited layer. The damaged seed layer was repaired using electroless plating. Cu re-covered the surface and the crystal structure of the seed layer was rebuilt and, finally, the filling characteristic was improved into superfilling in Cu electroplating for the damascene process. Electroless repairing, however, increased the seed roughness due to the low nucleation on the exposed barrier surface and the accompanying three-dimensional Cu growth. To refine the repairing process by inducing the nucleation on the barrier surface, Sn–Pd activation was adopted before the repair, and it reduced the surface roughness and improved the continuity of the seed layer effectively.
 [DOI: 10.1149/1.3291985]

Manuscript submitted October 27, 2009; revised manuscript received December 11, 2009. Published February 9, 2010.

Cu electroplating has been used in the damascene process for forming interconnects in microprocessors, mainly due to the superior capability in filling the recessed region. Generally, it requires a Cu seed layer, which provides nucleation sites for the formation of a continuous film.[1,2] Additionally, it reduces the potential drop originating from its own resistance and, accordingly, prevents a higher deposition rate on the substrate near the points electrically connected to the electron supplier for electroplating.[3,4] Moreover, the nature of the seed layer affects the resistivity, crystallinity, and adhesion of the electrodeposit.[5-8]

In submicrometer technology generations, the Cu seed layer is usually deposited using a physical vapor deposition (PVD) method. As the trench width decreases to the tens of nanometers range, it becomes more difficult to obtain a continuous and conformal seed layer on the trench wall, especially at the trench base. This is due to the directional deposition of PVD, which results in a "bottom void" during trench filling.[4] Moreover, the coverage of the seed layer becomes worse by the damage in the acidic plating electrolyte. The native Cu oxide formed on the seed layer is dissolved in the acidic electrolyte, resulting in defects in the seed layer.[4,8-10] Martyak and Ricou[2] observed seed layer damage in a sulfuric-acid-based electrolyte by applying 100 $\mu A/cm^2$ of anodic current on the seed layer.

Before adopting methods such as atomic layer deposition and electroless plating in the seed layer fabrication, seed layer repair has been suggested as a bridge between PVD and the methods mentioned. Seed layer repair is a technique that improves the continuity of the seed layer by connecting sparse parts of Cu seed through the addition of a few Cu layers. Electroless plating,[11] alkaline-based electroplating,[11,12] and low acid electroplating[10] have been reported as repairing methods.

This work is a fundamental study on the seed damage and its repair using electroless plating for the appropriate application of repairing in the damascene process. We caused damage to a seed layer via immersion in an acidic plating electrolyte and repaired it using electroless plating, and we observed changes in the properties of the seed layer and the effect on the subsequent electroplating for each treatment.

Experimental

Cu seed layers used in this study were 10, 30, and 50 nm thick and were formed on a nonpatterned Si wafer, which has the multilayers of PVD Ta (7.5 nm)/PVD TaN (7.5 nm). A patterned wafer, which has 55 nm width trenches with an aspect ratio of 3.5 and PVD Cu (7.5 nm)/PVD Ta (6 nm)/PVD TaN (1.5 nm)/Si multilayer, was also used in the trench-filling experiment. The wafer was dipped in a conventional sulfuric-acid-based solution for 300 s as a damaging process. The composition of the plating solution was $CuSO_4 \cdot 5H_2O$ (0.25 M), H_2SO_4 (1.0 M), NaCl (1 mM), poly(ethylene glycol) (PEG, 88 μM, Mw 3400, Aldrich), and bis(3-sulfopropyl) disulfide (SPS, 50 μM, Raschig GmbH). 1,2,3-Benzotriazole (BTA, 1 mM, Junsei) was added as a corrosion inhibitor. With 99.9% Cu wire and a saturated calomel electrode (SCE) as a counter electrode and a reference electrode, respectively, electroplating was performed at -200 mV (vs SCE) on a 1 cm^2 seed layer surface in the plating solution.

The damaged seed layer was repaired using Cu electroless plating, which was performed at 70°C in a solution containing $CuSO_4 \cdot 5H_2O$ (0.006 M), ethylenediaminetetraacetic acid (0.0077 M), paraformaldehyde [$(HCHO)_n$, 0.014 M], and KOH (0.069 M). Surface activation was attempted before electroless plating for the improvement of repairing results. Surface activation was carried out via Sn sensitization (in 0.03 M $SnCl_2$ and 1.94 M HCl solution for 120 s) and Pd activation (in 0.56 mM $PdCl_2$ and 0.08 M HCl solution for 20 s) as used for electroless plating on the Ta substrate.[13-15]

Four-point probe analysis (Chang Min Co., CMT-SR 1000N), a field-emission-scanning electron microscope (FESEM, JEOL, JSM-6330F), an X-ray photoelectron spectroscope (XPS, Kratos, AXIS), an X-ray diffractometer (XRD, Bruker, D8 Advance), and an atomic force microscope (AFM, Park SYSTEMS, XE-150) were used to analyze the change in the seed properties during the damage and the repair.

Results and Discussion

Figure 1 shows the changes in the surface morphology and the sheet resistance of the 10 nm thick seed layer during immersion in the plating electrolyte. It showed that the seed layer was severely damaged by the plating electrolyte, and the underlying barrier layer was exposed to the surface. The sharp increase in the sheet resistance after 200 s indicates that the seed layer became physically discontinuous. It is easily considered that the damage is caused by the dissolution of the native Cu oxide on the seed layer, as shown in the following reaction[4,9]

$$CuO + 2H^+ \rightarrow Cu^{2+} + H_2O \quad [1]$$

The pH at equilibrium of Eq. 1 is 4.83 (which can be calculated using standard molar Gibbs free energy of formation at $[Cu^{2+}] = 0.25$ M, 25°C). Because the pH of the plating electrolyte is 0.24, this is a thermodynamically spontaneous reaction. The change in the Cu surface resulted in defects at the surface and increased the sheet resistance of the seed layer. However, the dissolution of thenative oxide is unlikely to be the only one contributing to damage because

* Electrochemical Society Active Member.
** Electrochemical Society Student Member.
z E-mail: jjkimm@snu.ac.kr

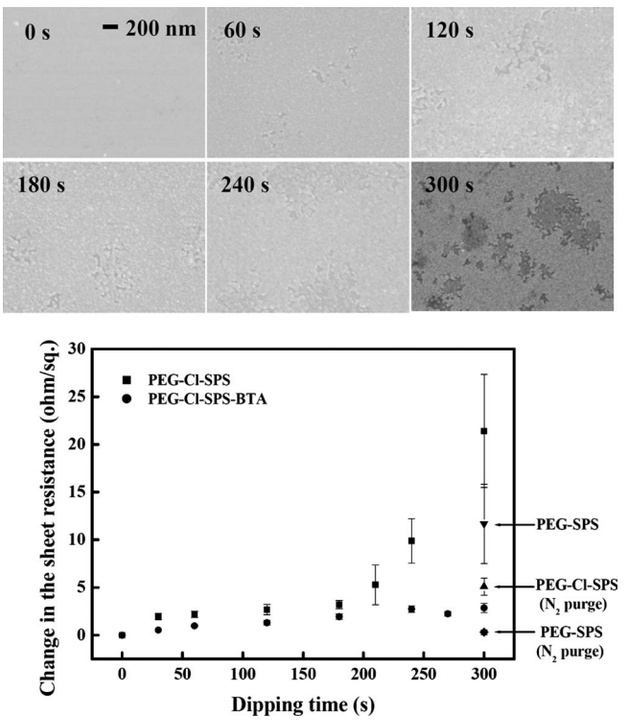

Figure 1. The changes in the surface morphology and the sheet resistance of 10 nm thick seed layer according to the immersion time in the plating electrolyte.

the native oxide formed on a 10 nm thick Cu seed layer was decomposed in a few tens of seconds in the acid solution.[16] Thus, if the damage were only due to the dissolution of the native oxide, deterioration would not continuously occur for 300 s. Moreover, the thickness of the native oxide layer has been reported to be normally less than 5 nm with the nonuniform nature, depending on the ambient oxidation condition such as relative humidity, temperature, and the oxidation time.[17,18] Therefore, dissolution of the native oxide may not be sufficient to expose the underlying layer. Some studies reported that metallic Cu can be dissolved by corrosion in the sulfuric acid containing oxidants such as Fe salt, dichromate, and dissolved O_2.[19-21] When BTA was added to the plating electrolyte to inhibit corrosion, the increase in the sheet resistance was almost completely suppressed over all dipping times. The small increase is certainly related to the dissolution of Cu oxide in the acidic solution. This indicates that the serious damage was mainly due to corrosion induced by oxidants, which damaged the seed layer as the immersion time increased. In this case, the oxidants in the plating electrolyte would be O_2 (which was dissolved in contact with air) and Cl ion (which was added as NaCl). To evaluate the effect of dissolved O_2, N_2 purging was conducted to remove dissolved O_2 before the seed layer was dipped in the electrolyte. In the purging, 99.9% N_2 gas was flowed in the electrolyte through a 0.5 cm diameter silicon tube with a flow rate of 100 mL/s. As shown in Fig. 1, when the plating electrolyte was purged with N_2 gas, the sheet resistance did not increase as much as the previous result. Similarly, the absence of Cl ions in the plating electrolyte also lessened the increase of the sheet resistance related to the damage. N_2-purged Cl-absent plating electrolyte as a combinational treatment made a very small increment as much as the BTA-containing electrolyte did. The corrosion caused by dissolved O_2 and Cl ion can be expressed as follows[21-23]

$$2Cu + 4H^+ + O_2 \rightarrow 2Cu^{2+} + 2H_2O \quad [2]$$

$$Cu + 2Cl^- \rightarrow CuCl_2^- + e^- \quad [3]$$

In summary, damage to the seed layer by the plating electrolyte occurs in two ways: the dissolution of native Cu oxide and corrosion caused by dissolved O_2 and Cl ion. The corrosion caused the damage to be more severe compared to the dissolution of the native oxide.

The changes in the composition and crystallinity of the seed layer due to the damage were observed using XPS and XRD analyses, as shown in Fig. 2. Before the immersion in the electrolyte, the XPS peaks of Cu(II) and the satellite corresponding to the native

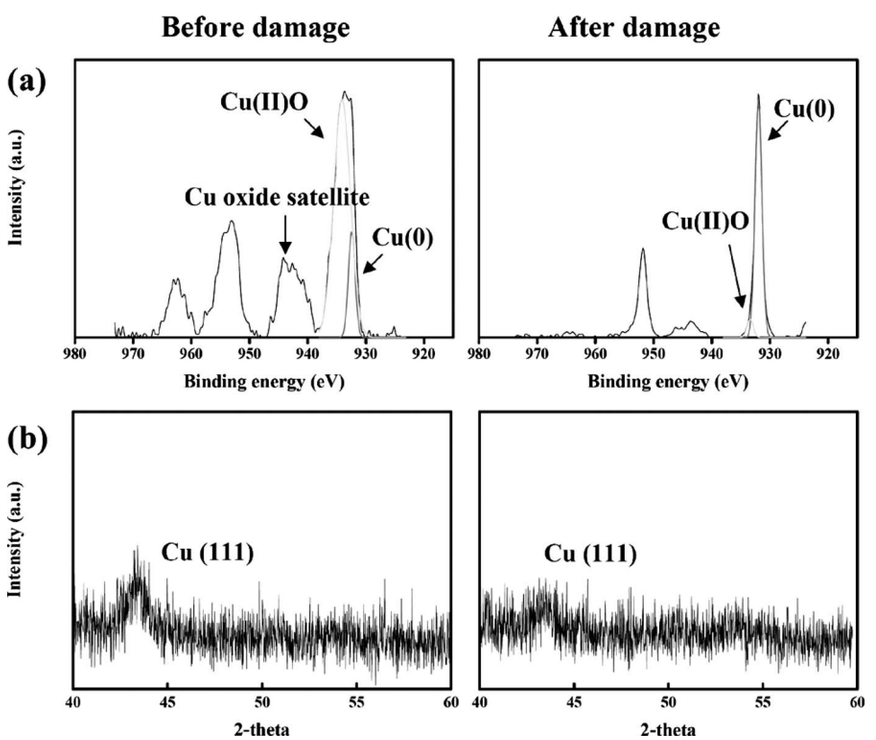

Figure 2. (a) Cu 2p 3/2 X-ray photoelectron spectrum and (b) X-ray diffraction spectra of 10 nm thick seed layer before and after immersion in the plating electrolyte.

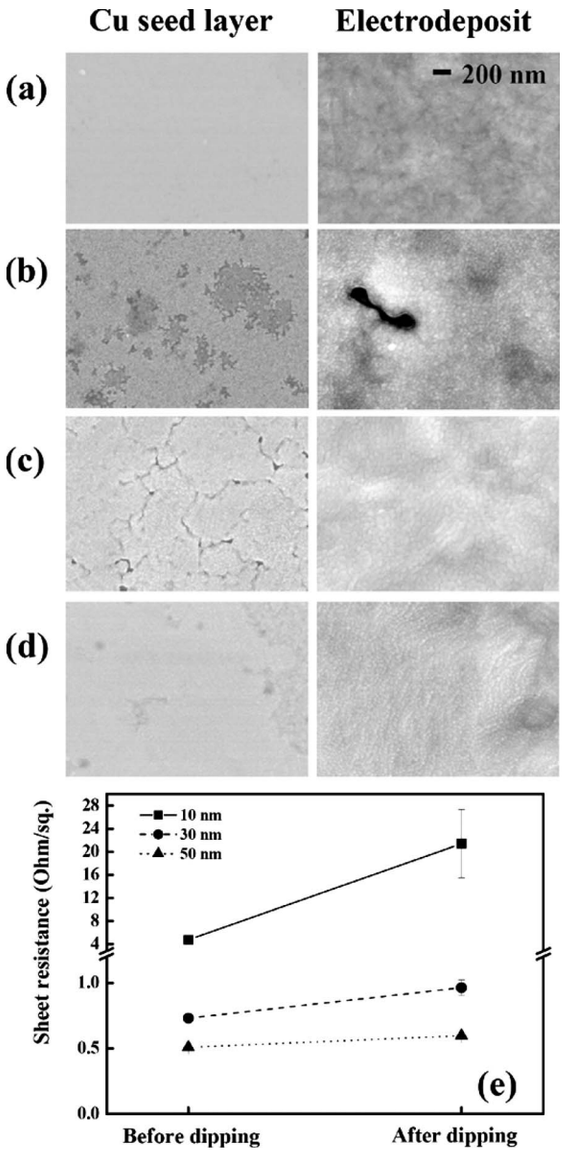

Figure 3. The relationship between the surface damage and the generation of defects in the electrodeposit according to the seed thickness: (a) As-prepared 10 nm thick seed, (b) damaged 10 nm thick seed, (c) damaged 30 nm thick seed, (d) damaged 50 nm thick seed, and (e) the change in the sheet resistance of the seed layer of various thicknesses with the damage. Electroplating was performed at −200 mV (vs SCE) for 30 s.

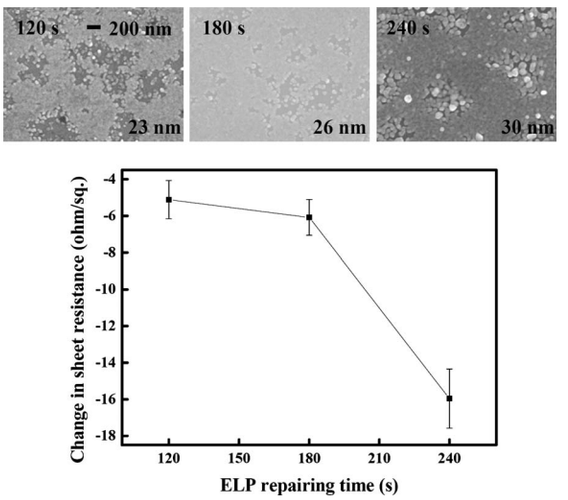

Figure 4. The changes in the surface morphology and the sheet resistance of 10 nm thick seed layer during seed layer repairing. The number at the bottom of each SEM image corresponds to seed thickness obtained from evaluating the step height in the line scan of AFM analysis.

oxide were observed (Fig. 2a). These became smaller after the immersion, which indicates the dissolution of the native oxide. The damage also changed the crystallinity of the seed layer. Figure 2b shows XRD spectra of the 10 nm thick Cu seed layer before and after the immersion in the electrolyte. Although the spectra show high levels of noise due to the thin seed layer, a (111) preferential orientation was detected on the seed layer. The intensity of the Cu(111) peak, however, was reduced after immersion in the plating electrolyte due to the dissolution of Cu accompanying the decrease in the thickness and the destruction of the crystal structure of the seed layer with the corrosion.

Figure 3 shows the surface damage and its effects on the subsequent electroplating with various seed thicknesses. Although a continuous electrodeposit film was obtained from the undamaged 10 nm thick seed layer (Fig. 3a), defects were visible in the electrodeposit on the damaged seed layer (Fig. 3b). As it is difficult for Cu to nucleate on the barrier layer exposed on the surface (due to the damage), uneven and sparse nuclei initially formed and, consequently, Cu growth progressed three-dimensionally, whereby Cu electrodeposit had a rough surface and many defects. Thicker seed layers were also damaged by the plating electrolyte, but the degree of damage was less severe than that of the 10 nm thick seed layer (Fig. 3c and d). As the seed layer became thicker, the sheet resistance increase associated with the damage became smaller (Fig. 3e). In consequence, defects were not generated after the plating on the seed layers with a thickness of over 30 nm. Conclusively, the damage to the seed layer caused to generate defects in the electroplating, and its effect, became serious as the seed layer became thinner in consistency with the shrinkage in the interconnect size.

The damaged seed layer was repaired using electroless plating. Figure 4 shows changes in the sheet resistance and the surface morphology of the 10 nm thick seed layer with the repair. During repair, the resistivity decreased sharply as the surface was re-covered with Cu, and the seed layer became continuous again. With 240 s of electroless plating, the sheet resistance reverted almost to the same value as that of the undamaged seed layer, and the surface was almost recovered. Figure 5 shows the reconstruction of the Cu(111) peak in the XRD analysis after the repair for 120 s. That is, the intensity of the Cu(111) peak decreased after damage and recovered after the repair, but the crystal orientation of the Cu seed layer remained unchanged.

Seed repairing was applied to a 55 nm width trench (Fig. 6). As shown in Fig. 6a and b, the seed layer was readily damaged by the plating electrolyte, whereby Cu did not superfill the trench (Fig. 6c). In contrast, when the electroless repairing was performed (for 60 s) before the immersion in the plating electrolyte, superfilling was successfully achieved in the trench (Fig. 6d).

In summary, seed layer repairing improves the continuity and crystallinity of the seed layer and the filling quality in the subsequent electroplating. However, it resulted in some roughening of the seed layer, as revealed by AFM analyses (Fig. 7). Before applying repair, the damaged recessed regions were found in AFM analyses as well as in FESEM analyses, and its depth was about 10 nm, equal to the total thickness of the seed layer, as shown in an AFM line scan (Fig. 7a). As the repair was performed on the damaged seed layer, the roughness increased to about 13 nm. This is due to the lack of Cu nucleation on the exposed barrier (Ta) surface. Therefore, Cu grew three-dimensionally only on the residual Cu surface (Fig. 7b and c). Three-dimensionally grown Cu regions appeared as domi-

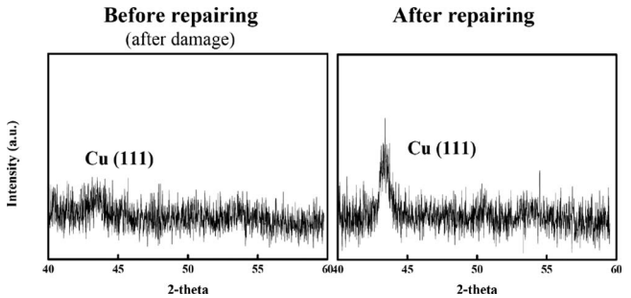

Figure 5. X-ray diffraction spectra of 10 nm thick Cu seed layer (a) before and (b) after seed layer repairing (for 120 s).

nant peaks in the AFM line scan and as white dots in the SEM image. These indicated that the recovery of the seed coverage was obtained by a three-dimensional and lateral growth of Cu at the boundary of the recessed region, whereby the roughness and thickness of the seed layer increased. Preferential growth of Cu at the boundary was shown as a bulge at the end of the recess in the AFM line scan. When the surface was almost completely covered with Cu after 240 s, the seed layer thickness increased to about 30 nm, which was deduced from evaluating the step height in the line scan.

As a feature of the dimension scale, a thin, continuous, and smooth seed layer becomes central to void-free gap filling. Therefore, the thickness and roughness of the seed layer should be maintained at a minimal value. In this sense, seed layer repairing should be allowed until the seed layer became continuous and, ideally, should be carried out in such a way that Cu is nucleated on the barrier surface and grows two-dimensionally to minimize roughening. To achieve the nucleation on the barrier layer and two-dimensional Cu growth, Sn–Pd activation was performed on the damaged seed layer. Sn–Pd activation is a surface treatment method used in Cu electroless plating to deposit Cu on Ta and TaN surfaces.[13-15] Figure 8 shows schematic diagrams of the repair process with and without the surface activation. When electroless repairing is performed on the damaged surface, Cu grows only where Cu already exists, resulting in the rough seed layer with incomplete

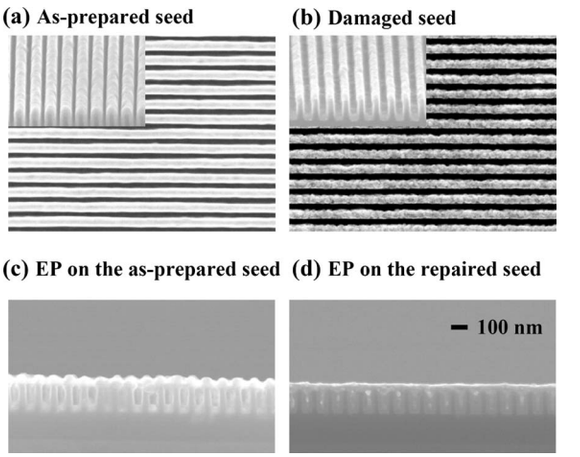

Figure 6. FESEM images of the seed layers, which were (a) as-prepared and (b) damaged, and electrodeposits on the seed layers which were (c) not repaired and (d) repaired (for 60 s) in the 55 nm trench. Electroplating was performed at −200 mV for 6 s with PEG–Cl–SPS additives.

Cu coverage. However, when surface activation is performed before electroless repairing, the Sn–Pd catalyst is formed on the barrier surface and allows nucleation of Cu as well as on Cu surfaces, resulting in a more continuous seed layer with less roughness.

Figure 9 shows FESEM and AFM images of the repaired seed layer using the surface activation as a pretreatment. The SEM image in Fig. 9a shows that the Sn–Pd particles were formed on the barrier surface, as observed in the AFM image. When electroless repairing was performed on the Sn–Pd particle-populated surface, it covered the surface with Cu perfectly even in just 30 s, with a low surface roughness of about 7 nm. This is a reduction of 40% in roughness compared to that of the repaired seed without activation (Fig. 9b-d). The rapid repairing using Sn–Pd activation was also adopted in trench filling (Fig. 10). As shown in Fig. 10a, repairing without Sn–Pd activation for 30 s was insufficient to guarantee superfilling in the subsequent electroplating. However, when activation was per-

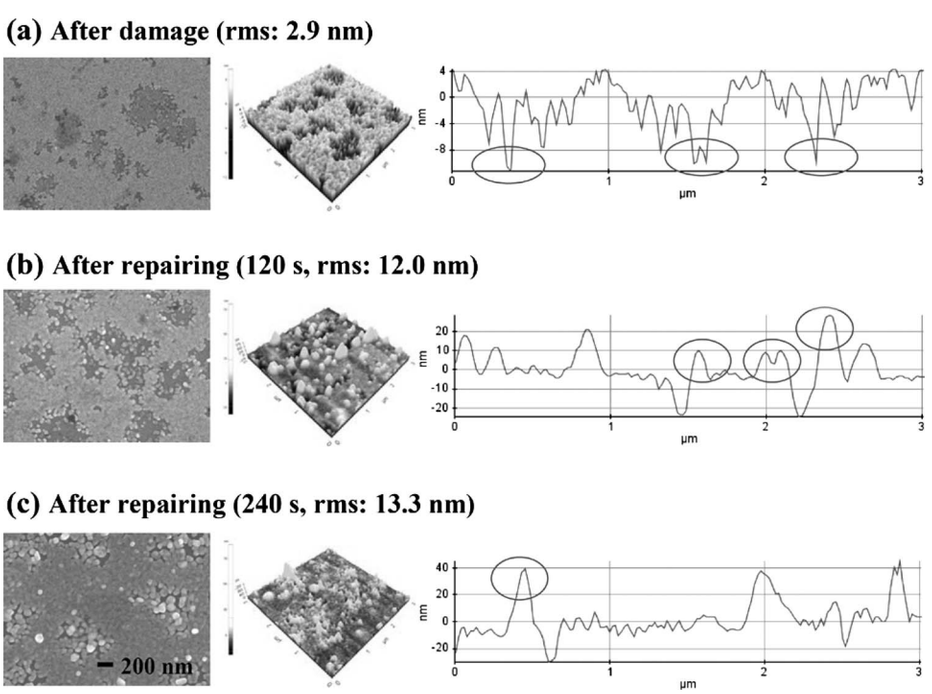

Figure 7. Surface images of FESEM analyses, and surface images and line-scan profiles of AFM analyses on the seed layers which were (a) damaged and [(b) and (c)] electrolessly repaired [for (b) 120 and (c) 240 s, respectively].

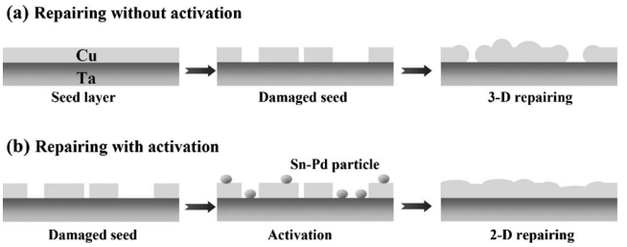

Figure 8. Schematic diagrams of repairing process of the seed layer using electroless plating (a) without and (b) with Sn–Pd surface activation.

formed before repairing, even a 10 s repair led to superfilling (Fig. 10b). The rapid repairing using Sn–Pd activation is meaningful not only because it could reduce the repairing time, but also because it could reduce the roughness and thickness of the seed layer after complete repairing. In the respect that seed repairing is a kind of bridging technique, these are favorable characteristics, as mentioned above. The reduction of repairing time is also meaningful in the aspect associated with the degradation of the exposed barrier (Ta) layer, which can be oxidized in the repairing solution. That is, rapid repairing can reduce the time for the exposure of Ta to the repairing solution and, consequently, reduce the chance of its oxidation.

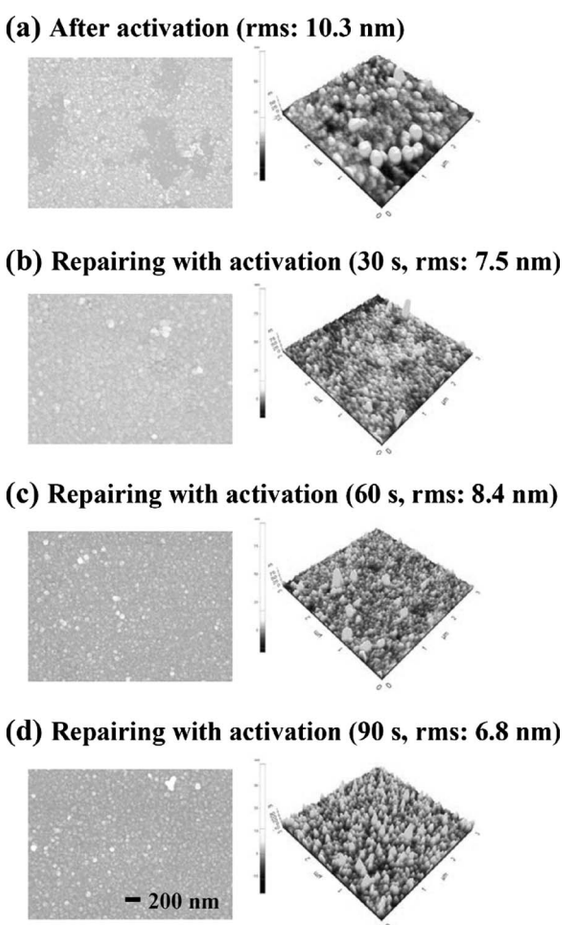

Figure 9. Surface images of FESEM and AFM analyses on the seed layers which were (a) activated and [(b)-(d)] electrolessly repaired [for (b) 30, (c) 60, and (d) 90 s, respectively] after Sn–Pd activation.

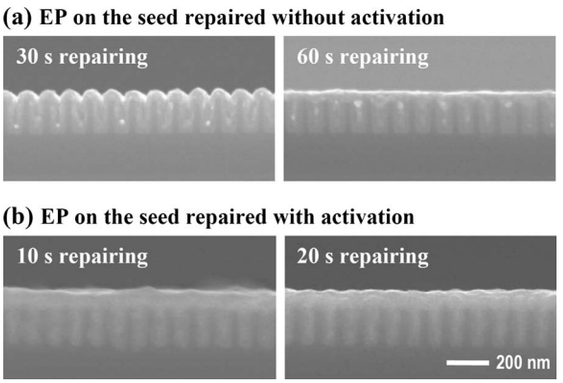

Figure 10. FESEM images of Cu electrodeposits on the seed layers which were repaired (a) without and (b) with Sn–Pd activation. Electroplating was performed at −200 mV for 6 s with PEG–Cl–SPS additives.

Conclusions

Damage to the Cu seed layer occurred due to the acidic plating electrolyte. This was associated with the dissolution of native Cu oxide and corrosion of Cu with the dissolved O_2 and Cl ions in the plating electrolyte. It increased the resistance and decreased the (111) crystallinity of the seed layer and defects in the electrodeposit. The damaged seed layer was repaired using electroless plating, and the original resistance and crystallinity were obtained. However, the roughness of the seed layer increased because of the three-dimensional growth of Cu, originating from the absence of nucleation on the barrier surface. This was remedied by applying a Sn–Pd activation. Sn–Pd activation before electroless repairing, which allowed Cu to nucleate on the barrier layer, resulted in a more rapid repair with reduced surface roughness. Because seed layer repairing is a supplemental method, it can be applied as long as it does not seriously change the properties of the seed layer.

Acknowledgments

This work was supported by the Korea Science and Engineering Foundation (KOSEF) through the Research Center for Energy Conversion and Storage (RCECS) and through the Nano R&D program funded by the Ministry of Education, Science and Technology (2009-0083223). It was also supported by a grant from the Fundamental R&D Program for Core Technology of Materials funded by the Ministry of Commerce, Industry and Energy, Republic of Korea.

Seoul National University assisted in meeting the publication costs of this article.

References

1. P. M. Hoffmann, A. Radisic, and P. C. Searson, *J. Electrochem. Soc.*, **147**, 2576 (2000).
2. N. M. Martyak and P. Ricou, *Mater. Sci. Semicond. Process.*, **6**, 225 (2003).
3. K. M. Takahashi, *J. Electrochem. Soc.*, **147**, 1414 (2000).
4. J. Reid, *Jpn. J. Appl. Phys., Part 1*, **40**, 2650 (2001).
5. K. Weiss, S. Riedel, S. E. Schulz, M. Schwerd, H. Helneder, H. Wendt, and T. Gessner, *Microelectron. Eng.*, **50**, 433 (2000).
6. J. J. Kim, S.-K. Kim, C. H. Lee, and Y. S. Kim, *J. Vac. Sci. Technol. B*, **21**, 33 (2003).
7. T. Hara and H. Toida, *Electrochem. Solid-State Lett.*, **5**, C102 (2002).
8. N. M. Martyak and P. Ricou, *Mater. Chem. Phys.*, **84**, 87 (2004).
9. J. Reid, S. Mayer, E. Broadbent, E. Klawuhn, and K. Ashtiani, *Solid State Technol.*, **43**, 86 (2000).
10. R. A. Mikkola and J. M. Calvert, U.S. Pat. 6,682,642 (2004).
11. T. Andryuschenko and J. Reid, in *IEEE International Interconnect Conference 2001*, IEEE, p. 33 (2001).
12. S.-W. Lee, F. G. Shi, and S. D. Lopatin, *Microelectron. J.*, **33**, 945 (2002).
13. C. H. Lee, S. H. Cha, A. R. Kim, J.-H. Hong, and J. J. Kim, *J. Electrochem. Soc.*, **154**, D182 (2007).
14. S.-Y. Chang, C.-J. Hsu, R.-H. Fang, and S.-J. Lin, *J. Electrochem. Soc.*, **150**, C603 (2003).
15. H.-H. Hsu, C.-W. Teng, S.-J. Lin, and J.-W. Yeh, *J. Electrochem. Soc.*, **149**, C143 (2002).

16. H. Majima, Y. Awakura, T. Yazaki, and Y. Chikamori, *Metall. Trans. B*, **11**, 209 (1980).
17. S. Suzuki, Y. Ishikawa, M. Isshiki, and Y. Waseda, *Mater. Trans., JIM*, **38**, 1004 (1997).
18. J. J. Kim and S.-K. Kim, *Appl. Surf. Sci.*, **183**, 311 (2001).
19. C. V. King and L. Weidenhammer, *J. Am. Chem. Soc.*, **58**, 602 (1936).
20. D. P. Gregory and A. C. Riddiford, *J. Electrochem. Soc.*, **107**, 950, and references therein (1960).
21. S. M. Mayanna and T. H. V. Setty, *Corros. Sci.*, **15**, 627 (1975).
22. S. M. Mayanna and T. H. V. Setty, *Proc. Indian Acad. Sci., Math. Sci.* **80**, 184 (1974).
23. A. Shaban, E. Kálmán, and J. Telegdi, *Electrochim. Acta*, **43**, 159 (1998).